

We are IntechOpen, the world's leading publisher of Open Access books Built by scientists, for scientists

6,900

Open access books available

186,000

International authors and editors

200M

Downloads

Our authors are among the

154

Countries delivered to

TOP 1%

most cited scientists

12.2%

Contributors from top 500 universities



WEB OF SCIENCE™

Selection of our books indexed in the Book Citation Index
in Web of Science™ Core Collection (BKCI)

Interested in publishing with us?
Contact book.department@intechopen.com

Numbers displayed above are based on latest data collected.
For more information visit www.intechopen.com



Advanced Filter Development for WiMAX Applications

*Kaixue Ma, Leyu Zhang and Kiat Seng Yeo

**School of Computer Science & Technology; Tianjin University, China
Nanyang Technological University (NTU), Singapore*

1. Introduction

Wireless communication continues to bring increased opportunities for the radio frequency (RF) component and test equipment manufacturers. For example, according to the IEEE.802.16-2004 standard [1] [2], frequency band of 2GHz~11GHz (see Figure 1 a)) is split into three different radio frequency bands, 2.4 GHz and 3.5 GHz for licensed bands and 5.8GHz for unlicensed, each of which has unique processing requirements that are incompatible with the other frequency bands. The result will allow manufacturers of RF components and test equipment to have their products used for mass deployment. The high linearity requirements of the WiMAX communication, for example 2.4 GHz and 3.5 GHz WiMAX communication, urge the test equipment can not only acquire the fundamental signal but also its' harmonics. High performance Bandstop filter, which needs high rejection of fundamend signal f_s and ultra-wide passband across the harmonic up to $5f_s$ as shown in Figure 1 b), is required according to the WiMAX equipment scheme, which will be introduced in Section II.

Bandstop filter is important in the filter family [3] [4]. It is used to reject some particularly strong interfering frequency and while passing through the rest. It is widely used in cable televisions, satellite communication systems, and other communication systems. In the family of bandstop filters, lumped elements or resistor-inductor- capacitor bandstop filter is commonly used. The disadvantages including relative large size, large power consumption and possible parasitic effect limit the utilizations above the multi-gigahertz range. In fact, most of the bandstop filters operating above multi-GHz range are built by distributed transmission lines [5-14]. The bandstop filter architectures of a transmission line coupled to a grounded bandstop resonator by capacitive gaps and by parallel-line coupling are given in [5] and [6] respectively. In [7], Bell uses the quarter-wavelength L-shape resonator configuration to build up the bandstop filters. Qian and Zhuang [8] introduce a complementary relationship between a dual-mode bandpass and bandstop waveguide filter and verified the relationship by experiments. Superconducting bandstop filters using the open-ended half wavelength resonator are reported in [9] and [10]. More recently, in [11], the traditional bandstop filter using two open-ended stubs [3] is modified to bended square shape and 50% size reduction is achievable. The compact size microstrip interdigital bandstop filter [12], which is realized by loading the interdigital capacitors on the

transmission line, is presented. A close loop ring coupling to CPW transmission line by transverse slot is used for bandstop filter by using micro-electro-mechanical systems (MEMS) technology as demonstrated in [13]. In [14], the synthesizing of bandstop filter based on transmission line model is demonstrated.

In this Chapter, the new application of the bandstop filter for the nonlinear measurement for WiMAX application is introduced. A physical based lumped circuit model introduced in [16] is used for the bandstop filter design and analysis. Bandstop filters operate in 2.5 GHz and 3.5 GHz licensed WiMAX bands are developed and the physical parameters of these filters are given in this Chapter. As shown in Figure 1 b), the high performance bandstop filter with the rejection of f_s more than 60dB and passband up to the fifth of the fundamental frequency are achieved simultaneously. The important leakage issue due to packaging is discussed and a solution for the packaging to avoid the leakage and further improve the performance is introduced. Additional work on WiMAX bandpass filter is also introduced. The Chapter is arranged as follows: Firstly, the application and the requirements of the bandstop filter in WiMAX test equipment based on nonlinear measurement scheme are introduced in Section II. In Section III, the step impedance resonator section with different electric parameters and the resonant characteristics are investigated by using the circuit model. In Section IV, the step impedance resonator sections are used to build the 2.4 GHz and 3.5 GHz bandstop filter. 2.4 GHz and 3.5 GHz filters with good performance for WiMAX equipment are verified by experiments. In Section V, the leakage issues are investigated and the packaging free of leakages is designed and implemented. In section VI, the recent development work on 2.4GHz and 3.5GHz WiMAX bandpass filters is illustrated for WiMAX application. Finally, the conclusion is given in Section VII.

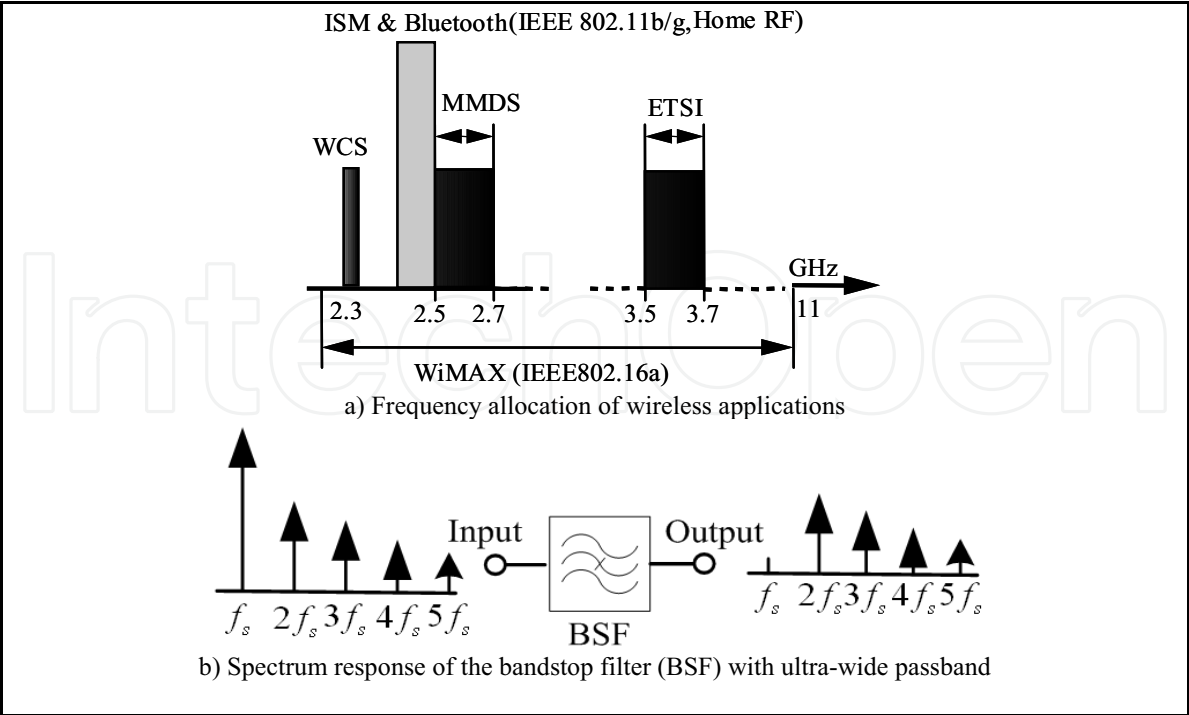


Fig. 1. Application requirements of the proposed bandstop filter

2. bandstop Filter Application in WiMAX Equipment

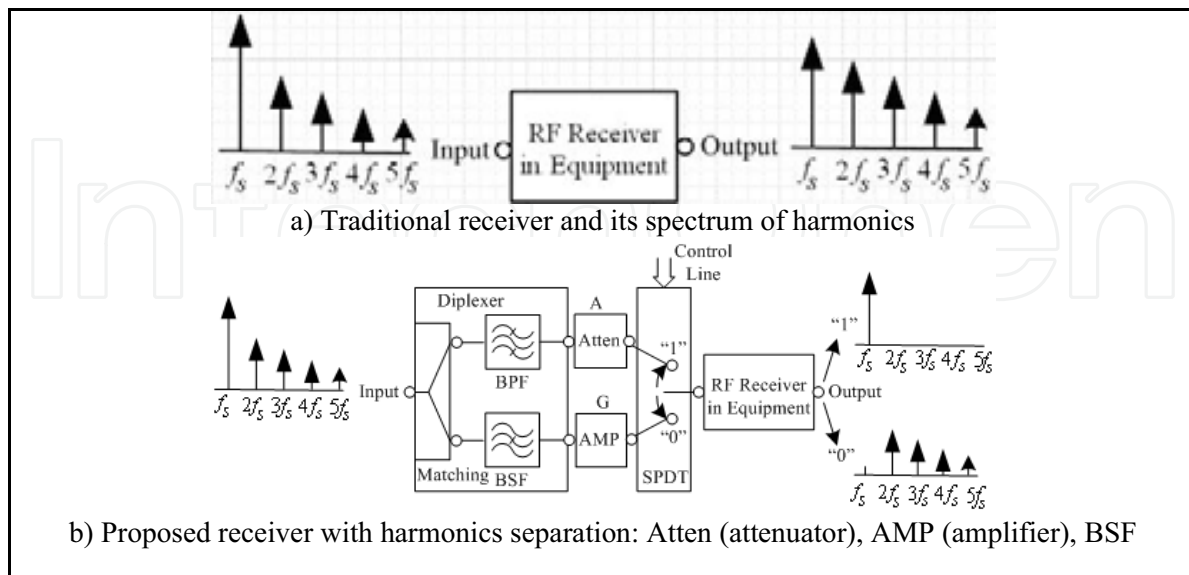


Fig. 2. Receiver front-end with/without harmonics separation

In nonlinear measurements such as measurement of WiMAX power amplifier or communication system, the equipment receiver is important to accurately capture the information of the device under test (DUT). To avoid the nonlinear effects generated from the equipment receiver itself, which will increase the errors in measurement, both the fundamental signal and its harmonics should be within the linear dynamic range of the equipment receiver. However, the fundamental signal has higher power level while its harmonics have relative lower power level. The limited dynamic range of the equipment receiver becomes a challenge to handle these two extreme power level conditions simultaneously. As shown in Figure 2 a), when the power level difference of the fundamental signal and its harmonics is larger than the dynamic range of broadband equipment receiver, the results from the output of equipment receiver will be either one of these two cases: case 1, only the fundamental signal is obtained and the harmonics information cannot be captured accurately due to the sensitivity of the receiver. Case 2, the fundamental signal will be suppressed and the harmonic will be increased due to the compression point of the equipment receiver itself).

In order to solve the above problems, the system scheme shown in Figure 2 b) is introduced to separate the fundamental signal and its harmonics. The fundamental signal, which has higher power level, goes to the bandpass filter and then compresses the power level of A dB by an attenuator. On the other hand, the harmonics with lower power level below the minimum receivable power level go through the bandstop filter and then are amplified by a low noise amplifier with a gain of G dB. Finally, the attenuated fundamental signal and the amplified harmonics are selected by the single-pole-double-throw (SPDT) switch and sent to equipment receiver (or are combined by a power combiner and send these signals to the equipment receiver). By doing so, the theoretical dynamic range of the equipment receiver can be increased by around A plus G dB. As in the system shown in Figure 2 b), to

achieve accurate measurements of the nonlinear characteristics, the performance of the bandstop filter is very important. Thus, the high rejection stopband, to avoid the fundamental signal entering into the harmonic channel, and ultra-wide passband, to capture the harmonics up to fifth for nonlinear measurement, are required.

3. Step Impedance Resonator Section Model

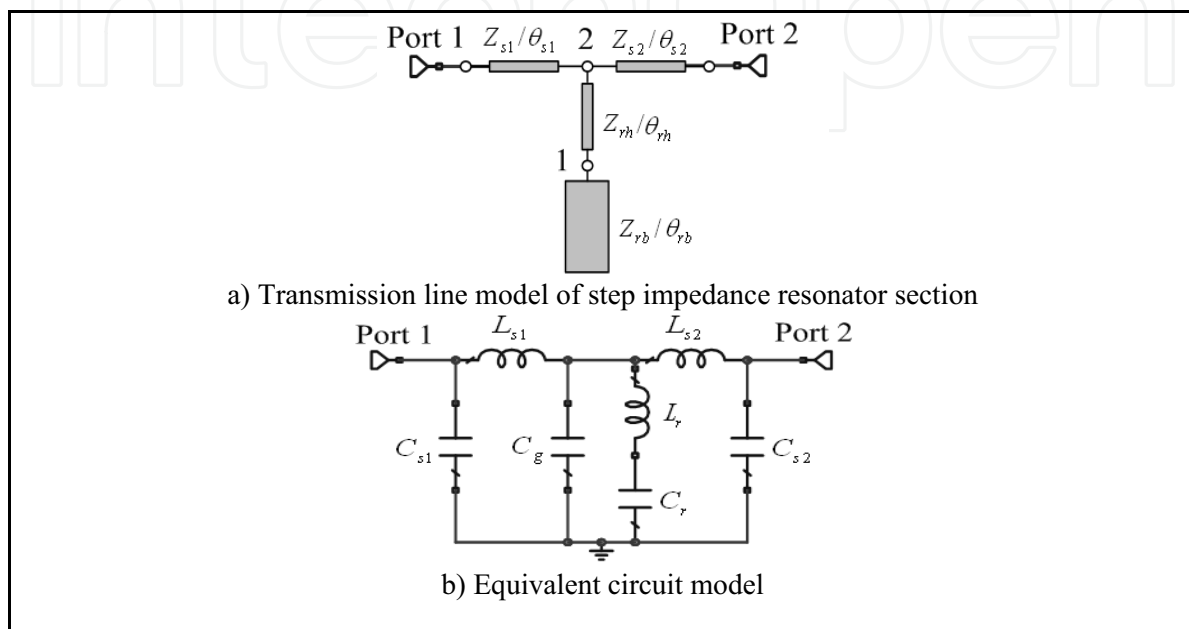


Fig. 3. Transmission line model and equivalent circuit of step impedance resonator section

The fundamental prototype block named step impedance resonator section for the bandstop filter is shown in Figure 3. It consists of a step impedance resonator and two matching section lines. The step impedance resonator is formed by an open stub (a characteristic impedance of Z_{rh} and electric length of θ_{rh}) connected in serial with a high impedance section (a characteristic impedance of Z_{rb} and an electric length of θ_{rb}). The two matching section lines with characteristic impedance and electric length of (Z_{s1}, θ_{s1}) and (Z_{s2}, θ_{s2}) respectively are used for source and load (source impedance Z_s and load impedance Z_L) matching at node "1" and "2" respectively. The input impedance of the step impedance resonator at node "2" can be given as:

$$Z_{SIR} = \frac{1 + s^2 L_r C_r}{s(C_r + C_g + s^2 L_r C_r)} \quad (1)$$

$$C_r = C_o + C_h \quad (2)$$

$$C_g = C_{s1} + C_{s2} + C_h \quad (3)$$

$$C_h = j(1 - \cos \theta_{rh}) / (s Z_{rh} \sin \theta_{rh}) \quad (4)$$

$$L_r = j Z_{rh} \sin \theta_{rh} / s \quad (5)$$

$$C_{s1} = j(1 - \cos \theta_{s1}) / (s Z_{s1} \sin \theta_{s1}) \quad (6)$$

$$C_{s1} = j(1 - \cos \theta_{s2}) / (sZ_{s2} \sin \theta_{s2}) \quad (7)$$

$$C_o = jZ_{rb} \tan \theta_{rb} / s \quad (8)$$

$$L_{s1} = jZ_{s1} \sin \theta_{s1} / s \quad (9)$$

$$L_{s2} = jZ_{s2} \sin \theta_{s2} / s \quad (10)$$

where $s = j\omega$ (ω is the angular frequency). The fundamental resonance condition is when the input impedance is equal to zero. Thus the resonance is constrained by the equations

$$f_r = 1 / (2\pi \sqrt{L_r C_r}) \quad (11)$$

$$f_p = 1 / 2\pi \sqrt{(C_g + C_r) / (L_r C_r)} \quad (12)$$

The above model-based derivation is convenient for the initial design of the filter. To get the frequency response for the whole frequency range, the two-port network parameters are used and the transfer matrix of the model in Figure 3 b) can be calculated by

$$\begin{bmatrix} T_{11} & T_{12} \\ T_{21} & T_{22} \end{bmatrix} = \begin{bmatrix} 1 & 0 \\ sC_{s1} & 1 \end{bmatrix} \begin{bmatrix} 1 + \frac{sL_{s1}}{Z_{sir}} & \frac{s^2 L_{s1} L_{s2}}{Z_{sir}} + s(L_{s1} + L_{s2}) \\ \frac{1}{Z_{sir}} & 1 + \frac{sL_{s2}}{Z_{sir}} \end{bmatrix} \begin{bmatrix} 1 & 0 \\ sC_{s2} & 1 \end{bmatrix} \quad (13)$$

and

$$T_{11} = 1 + s^2 C_{s2} (L_{s1} + L_{s2}) + (sL_{s1} + s^3 C_{s2} L_{s1} L_{s2}) / Z_{sir} \quad (14)$$

$$T_{12} = s(L_{s1} + L_{s2}) + s^2 L_{s1} L_{s2} / Z_{sir} \quad (15)$$

$$T_{21} = sC_{s1} + (1 + s^2 L_{s1} C_{s1}) / Z_{sir} \quad (16)$$

$$T_{22} = 1 + s^2 C_{s1} (L_{s1} + L_{s2}) + (sL_{s2} + s^3 C_{s1} L_{s1} L_{s2}) / Z_{sir} \quad (17)$$

The transmission and reflection characteristics can be determined by

$$S_{21} = \frac{2}{2T_{11} + T_{12} / Z_0 + T_{21} Z_0} \quad (18)$$

$$S_{11} = \frac{T_{12} / Z_0 - T_{21} Z_0}{2T_{11} + T_{12} / Z_0 + T_{21} Z_0} \quad (19)$$

When $\theta_{ru} = \theta_{rb} = \theta_r$, the second harmonic or spurious resonance occurs with following constraint

$$f_{r2} / f_{r1} = (180 - \theta_r) / \theta_r \quad (20)$$

where f_{r1} and f_{r2} are the fundamental resonant frequency and the second harmonic respectively.

It is found that the two matching section lines mainly affect the matching condition and have little effect on the resonant frequencies. Thus, the two section lines are fixed ($Z_{s1} = Z_{s2} = 50\ \Omega$, $\theta_{s1} = \theta_{s2} = 12^\circ$). The simulation results of five different conditions are compared in Figure 4 (All of the impedances are in Ω and all of the electric lengths are in degrees). As illustrated in Figure 4, the fundamental resonant frequency $f_{r1} = 1\text{ GHz}$ for the cases of a), b) c), d), e) is chosen for the convenience of comparison. It is clear that the smaller the ratio of Z_{ru}/Z_{rb} , the shorter the electric length is needed for the same operating frequency of 1 GHz (i.e. for the same operating frequency, the size of the step impedance resonator becomes compact with reduced Z_{ru}/Z_{rb}). On the other hand, the first harmonic f_{r2} depends on both the impedance ratio Z_{ru}/Z_{rb} and the electric lengths θ_{rb} and θ_{ru} . For the one special case, when the $Z_{ru}/Z_{rb} = 1$, the fundamental resonant frequency occurs at $\theta_{ru} = \theta_{rb} = 45$ and the first harmonic occurs at three times of the fundamental operating frequency. For another special case $\theta_{ru} = \theta_{rb} = \theta_r$, the relationship between the fundamental operating frequency and its first harmonic is constrained by equation (19).

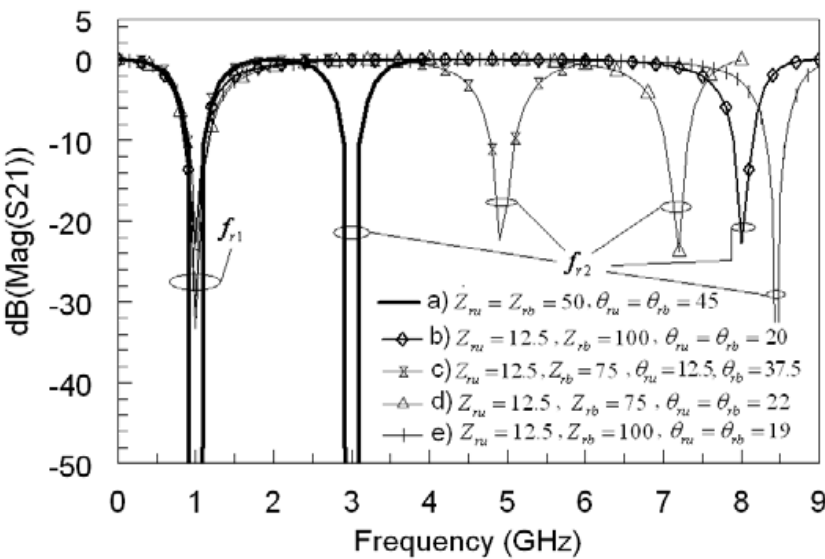


Fig. 4. Simulated results of the SIRS with different electric parameters

4. Design of filters for WiMAX equipment

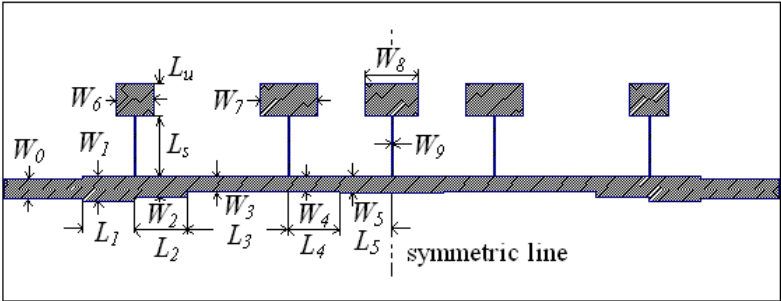


Fig. 5. Configuration of the proposed Microstrip bandstop filter

By understanding the characteristic of the step impedance resonator section, the multi-stage cascaded step impedance resonator sections can be used to build the bandstop filters shown in Figure 5 for WiMAX application introduced in Section II. According to the application requirements of the WiMAX equipment in Figure 1 and Figure 2, two bandstop filters are built for 2.4 GHz and 3.5 GHz WiMAX bands respectively. The fifth-order bandstop filter is formed by cascading five step impedance resonator sections using the cascade procedure in [15]. The electric parameters according to different step impedance resonator sections are synthesized and presented in [16] with consideration of the required total performance. The Rogers substrate RO3003 with dielectric constant of 3.0 has a substrate thickness of 20mil. The planar microstrip line is chosen for the design. The circuit simulator and Moment EM simulator in ADS 2005A are used to optimize the physical parameters for the 2.4 GHz and 3.5 GHz WiMAX filters. The dimensions of 2.4 GHz filter are: $W_0=1.26$ mm, $W_1=1.49$ mm, $L_1=4.77$ mm, $W_2=1.23$ mm, $L_2=5.24$ mm, $W_3=0.75$ mm, $L_3=10.9$ mm, $W_4=0.88$ mm, $L_4=4.64$ mm, $W_5=0.91$ mm, $L_5=6.1$ mm, $W_6=2.72$ mm, $L_u=3.59$ mm, $L_s=6.3$ mm, $W_7=3.91$ mm, $W_8=2.75$ mm and $W_9=0.1$ mm. The dimensions of 3.5 GHz filter are: $W_0=1.26$ mm, $W_1=1.6$ mm, $L_1=3.31$ mm, $W_2=1.4$ mm, $L_2=3.31$ mm, $W_3=1.0$ mm, $L_3=6.7$ mm, $W_4=1.0$ mm, $L_4=3.83$ mm, $W_5=1.04$ mm, $L_5=3.54$ mm, $W_6=2.51$ mm, $L_u=2.32$ mm, $L_s=4.07$ mm, $W_7=3.61$ mm, $W_8=3.74$ mm and $W_9=0.1$ mm.

In Figure 6 and Figure 7, the simulated and the measured results of the 2.4 GHz and 3.5 GHz filters without packaging housing are compared respectively. Both of the results agreed well in the passband as well as in the stopband. Both the 2.4 GHz and 3.5 GHz bandstop filters have the 3dB rejection band of 1.8~3.3 GHz and 3~5 GHz respectively, pass band ranges of DC~13.5 GHz and DC~21 GHz (except the stopband range) respectively. In the stopbands of 2.3~2.85 GHz and 3.4~4.1 GHz, the rejections are better than 60dB for both filters. The center frequency of the second stopband appears at as high as 6.2 times (15 GHz) and 6.3 times (22 GHz) of that of the fundamental stopband respectively. The board sizes of the 2.4 GHz and 3.5 GHz filters are only 74 mm by 35 mm ($0.6\lambda_0 \times 0.28\lambda_0$, λ_0 is the free space wavelength at center operating frequency) and 52 mm by 30 mm ($0.6\lambda_0 \times 0.34\lambda_0$) respectively.

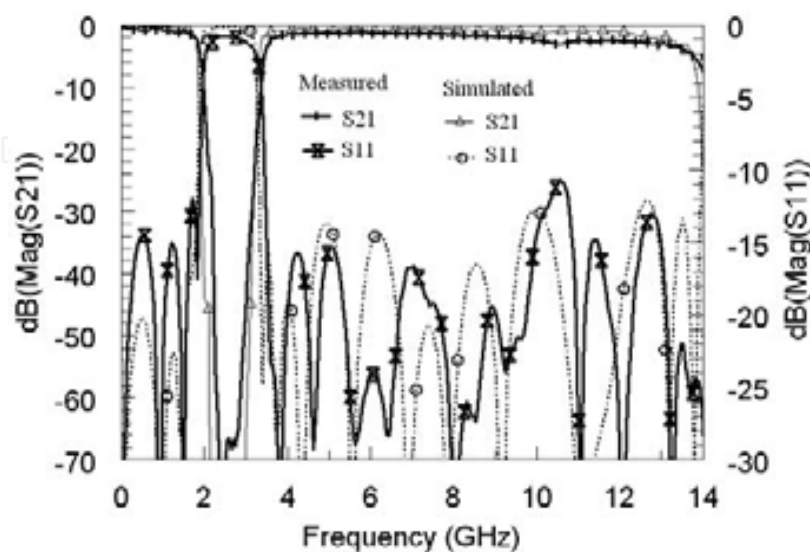


Fig. 6. Results of 2.4 GHz filter without metal housing

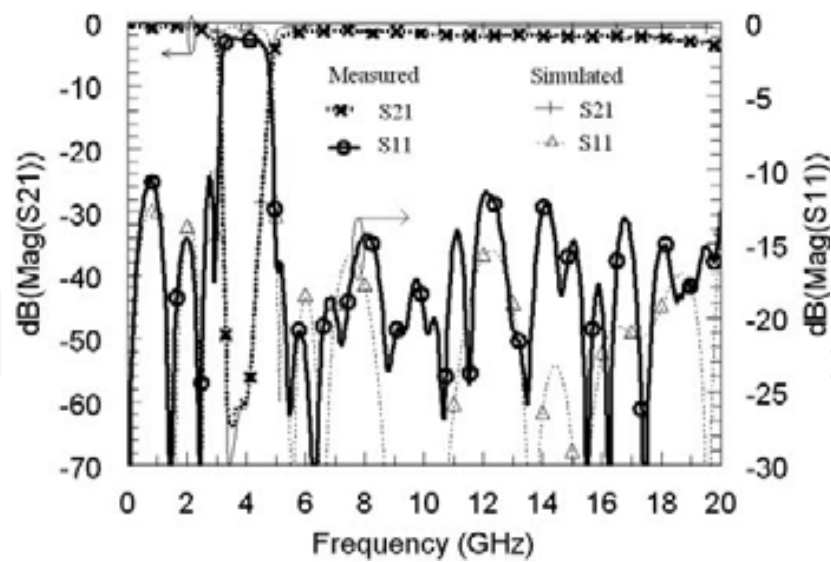


Fig. 7. Results of 3.5 GHz filter without metal housing

5. Packaging Related Issues

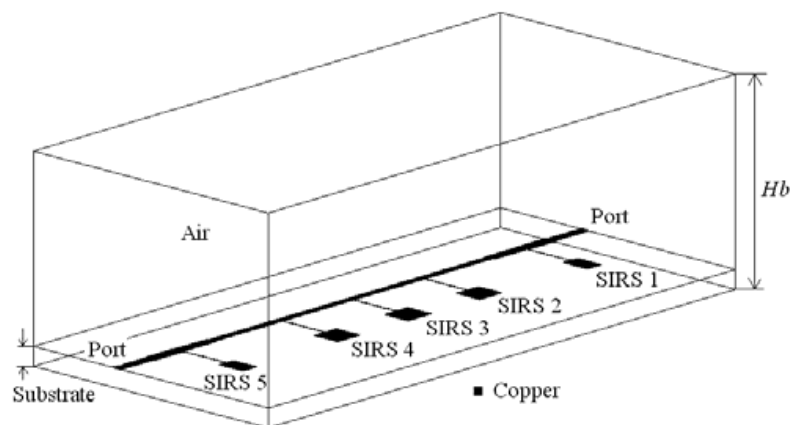


Fig. 8. Perspective view of the bandstop filter in metal housing SIRS (step impedance resonator section)

Electromagnetic compatibility/Electromagnetic Interference (EMC/EMI) control in the test equipment is important. Therefore, the modules in the equipment such as mixer, filter and amplifier, are required to be well shielded to avoid unwanted radiation and interference. The WiMAX filters introduced in Section IV has to be packaged for the equipment use. The perspective view of a 2.4 GHz WiMAX filter in the 3D metal housing of using the Sonnet EM simulator environment is shown in Figure 8. The metal house has a length of 74 mm, a width of 35 mm and a height of H_b . The 2.4 GHz WiMAX filter with five step impedance resonator section is denoted in the dark area. The leakage modes exist in the passband when the metal shielding house is introduced. The dip points (DPs) due to leakages in the metal housing appear in the pass band as the three cases of $H_b=5$ mm, 12 mm, and 15 mm shown in Figure 9. The dip points in the loss factor curves $(1-|S_{11}|^2-|S_{21}|^2)$ in Figure 8 are formed by leakages due to the metal housing. When the multiple step impedance resonator sections from 1 to 5 are cascaded, the multiple conductors in parallel may generate unwanted

leakage wave as in [17-21]. The leakage wave excites the waveguide cavity modes [17] of the metal housing and causes the dip points in the passband of the filter. Compared to the results of the same filter without metal house (which is free of leakage in the passband) in Figure 6 and Figure 7, the packaging of the filter through the metal housing deteriorates the performance of the pass band and causes the filter unsuitable for wide passband operation to be used in WiMAX test equipment. On the other hand, if the unpackaged filters are used, EMI/EMC requirements for the WiMAX test equipment may not be met.

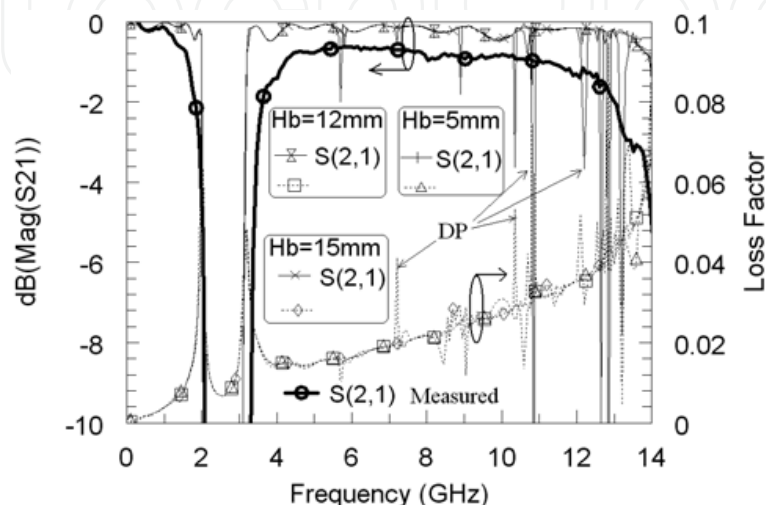


Fig. 9. Results of 2.4 GHz filter with/without metal housing

Through the experimental investigation, it is found that the issue can be solved by using the absorber material SS-6M from Emerson & Cuming. The absorber material attached inside metal cover changes the boundary condition of the metal housing. It is interesting that after packaging using the metal housing with absorber, the dip points in the passband no longer exist as measured result shown in Figure 9. Meanwhile, insertion loss in filter passband is also improved dramatically. The measured results of the 2.4 GHz and 3.5 GHz bandstop filters with and without housing are compared in Figure 10 and Figure 11 respectively. For the 2.4 GHz filter, the insertion loss including the SMA connector loss is less than 2.0 dB (most of the frequency range is less than 1 dB). Compared to the results of the 2.4 GHz filter without packaging, the proper packaging can reduce the insertion loss up to 0.5 dB at higher passband. For the 3.5 GHz filter, the improvement of the insertion loss with proper packaging is up to 1 dB at certain frequency range. In general, the proper packaging not only overcomes the leakage issue but also improves the passband performance. The packaging doesn't degrade the performance of the stopband as the measured group delays (GD) of the fifth-order filters are shown in Figure 12. The group delays in the passband are almost constant. The resonances occur in the stopband and the passband is a traveling-wave. The group delay variations of ± 0.5 ns are good for communication systems with high data rate or high linearity requirement. The photographs of the 2.4 GHz and 3.5 GHz WiMAX filter samples are shown in Figure 19. These two types of filter are now applied to the Agilent Technologies WiMAX test equipment.

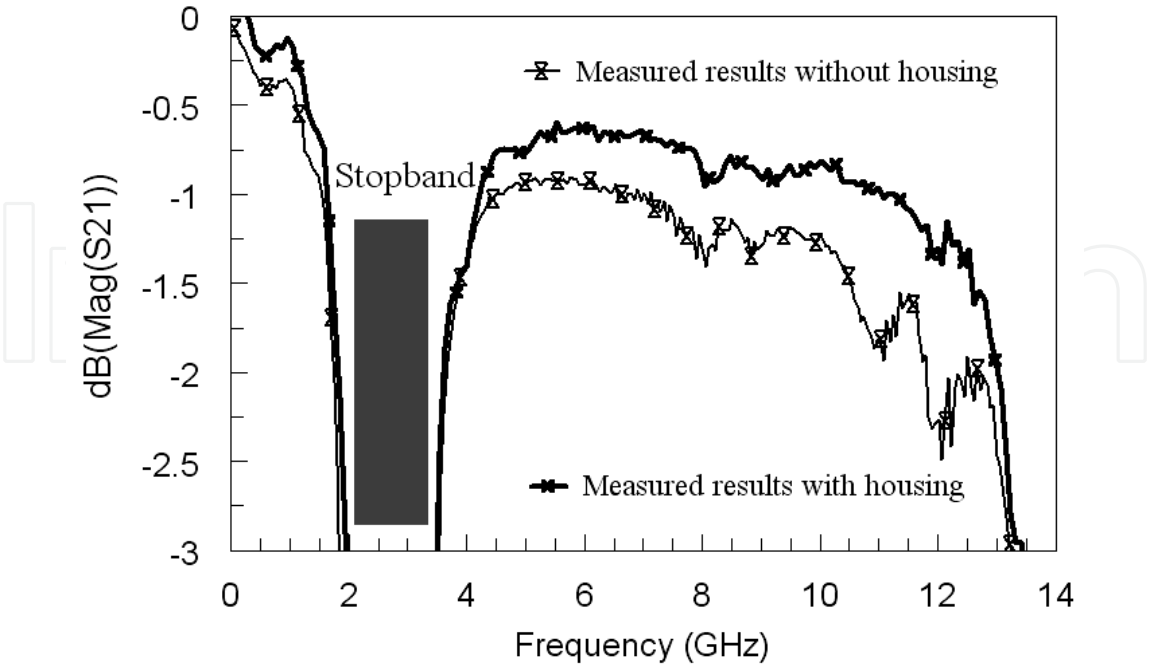


Fig. 10. Comparison of 2.4 GHz filter with/without metal housing

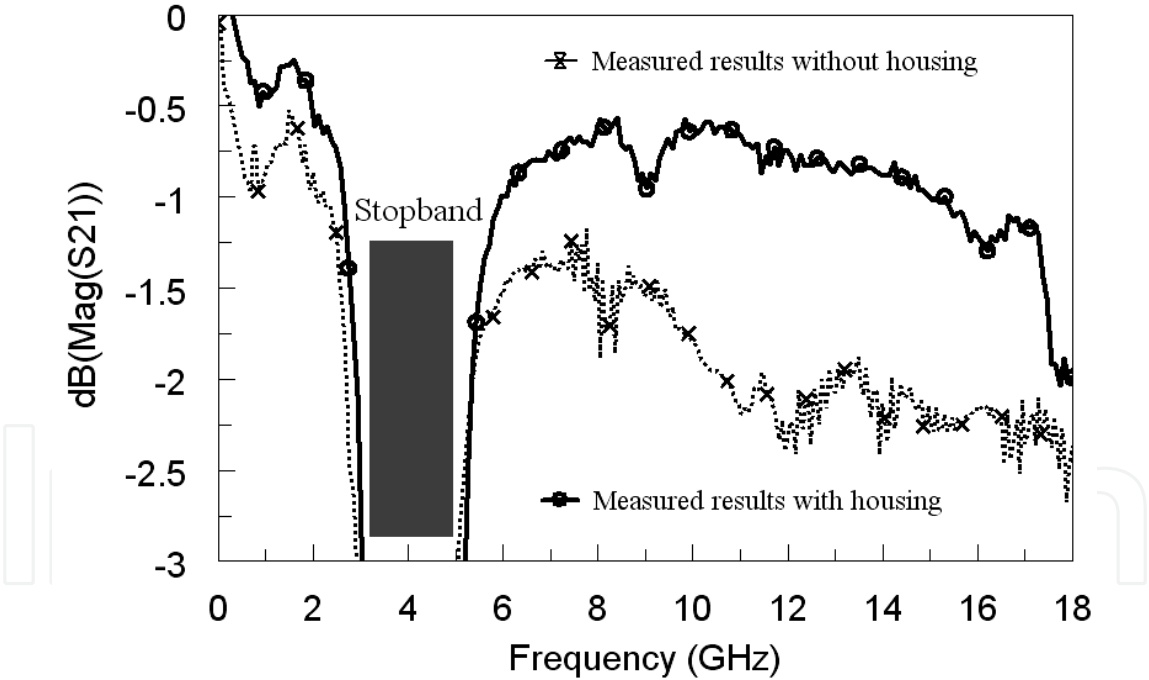


Fig. 11. Comparison of 3.5 GHz filter with/without metal housing

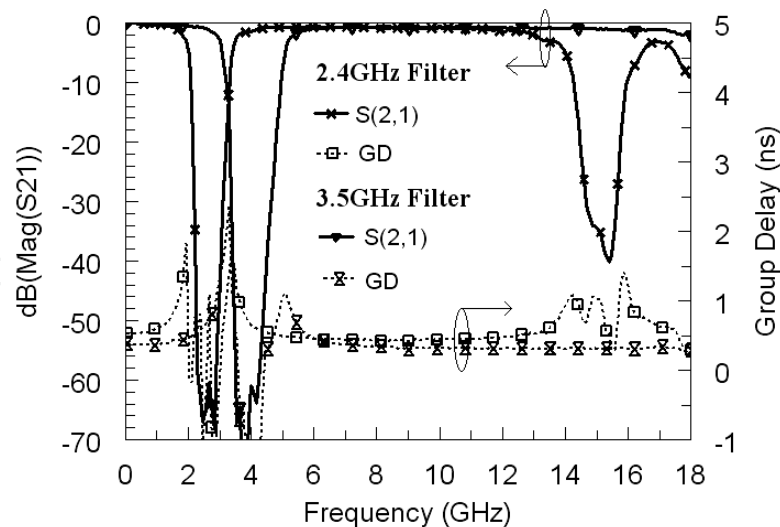


Fig. 12. Measured results of 2.4 GHz and 3.5 GHz filters with proper packaged metal housing

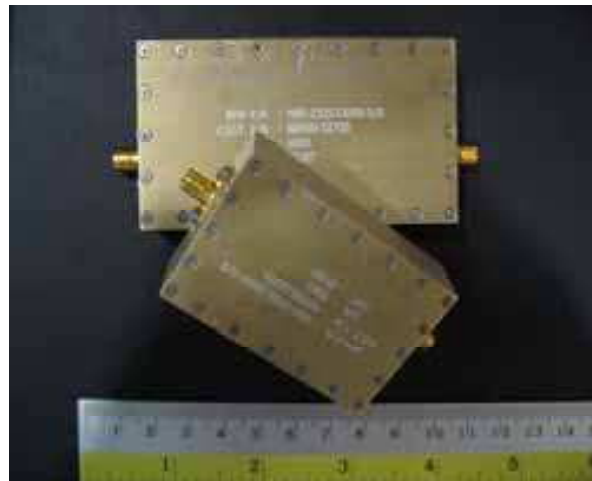


Fig. 13. Photographs of 2.4 GHz and 3.5 GHz WiMAX filter samples

6. Miniaturized Surface Mounted Bandpass Filter

In the application of WiMAX frontend, a bandpass filter is required to define the communication channel inside of the frontend and avoid the interferences from and to the other wireless communication applications. The portability and high linearity of the WiMAX terminal requires bandpass filter has a compact size, low cost and high performance. It is known that the miniaturization is the trend and designing compact passive devices is the challenging. Obviously, it would be impossible to face the challenging without novel design methodologies. Mainly, the electromagnetic (EM) characteristics determine the performance and size of the distributed transmission line filters. By investigating the EM characteristics of the circuits, different approaches, which form the basis of bandpass filters, need to be used for this target. Below shows parts of bandpass filters with high power handling, miniaturized size and high performance for WiMAX application multilayer through innovate use of multilayer technology. The focus is still on 2.4GHz and 3.5GHz WiMAX band.

a) 2.4GHz WiMAX bandpass filters

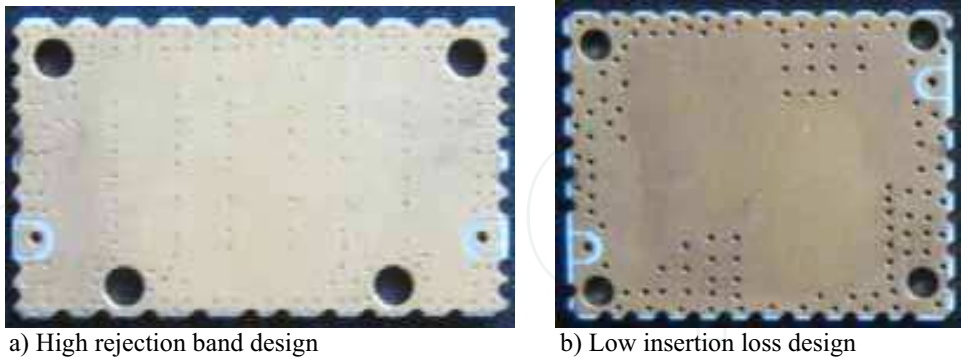


Fig. 14. Photographs of 2.4 GHz WiMAX filter samples

The band pass filter in Figure 14 a) has unique performances with pass band from 2.2GHz~2.6GHz with minimum insertion loss less than 2dB and ultra wide stop band from 2.9GHz to 10GHz as the measured results shown in Figure 15. The stop band rejection is better than 50dB from 3.7GHz to 7.7GHz. The band pass filter has much compact size of 29mm X 19mm X 1.5 mm³. The other strength is the packaging format of SMT which is convenient for integration.

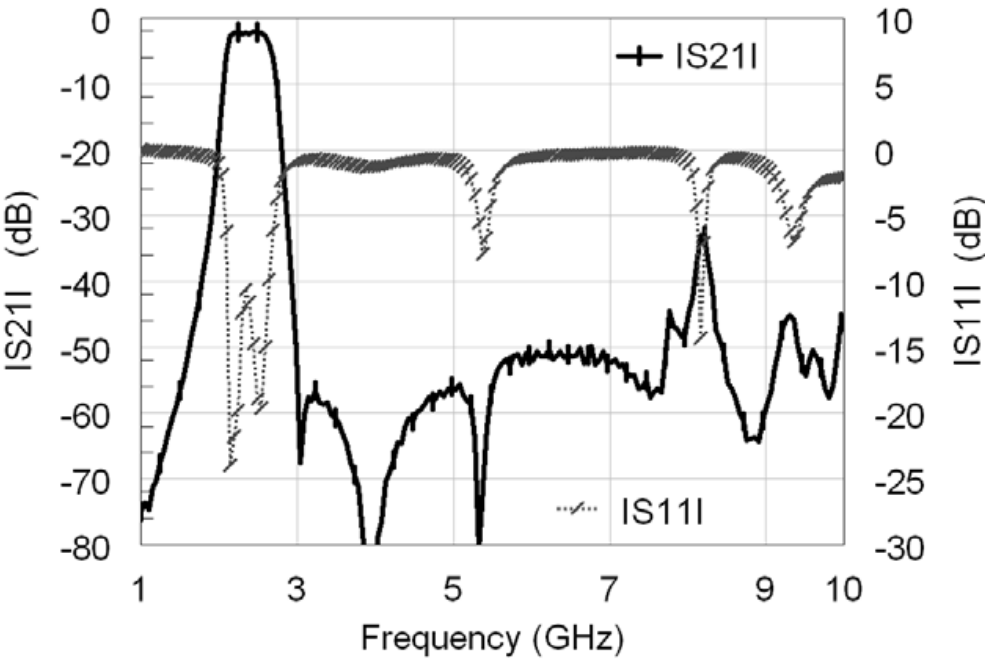


Fig. 15. Measured results of 2.2~2.6GHz high rejection WiMAX bandpass filter

The band pass filter in Figure 14 b) has unique performances with pass band from 2.2GHz~2.7GHz with minimum insertion loss less than 1dB and ultra wide stop band from 3GHz to 7.7GHz as the measured results shown in Figure 16. The stop band rejection is better than 50dB from 3.7GHz to 7.7GHz. The band pass filter has much compact size of 24.5mm X 19.5mm X 1.5 mm³. The other strength is the packaging format of surface mounting which is convenient for integration and free of RF power leakage.

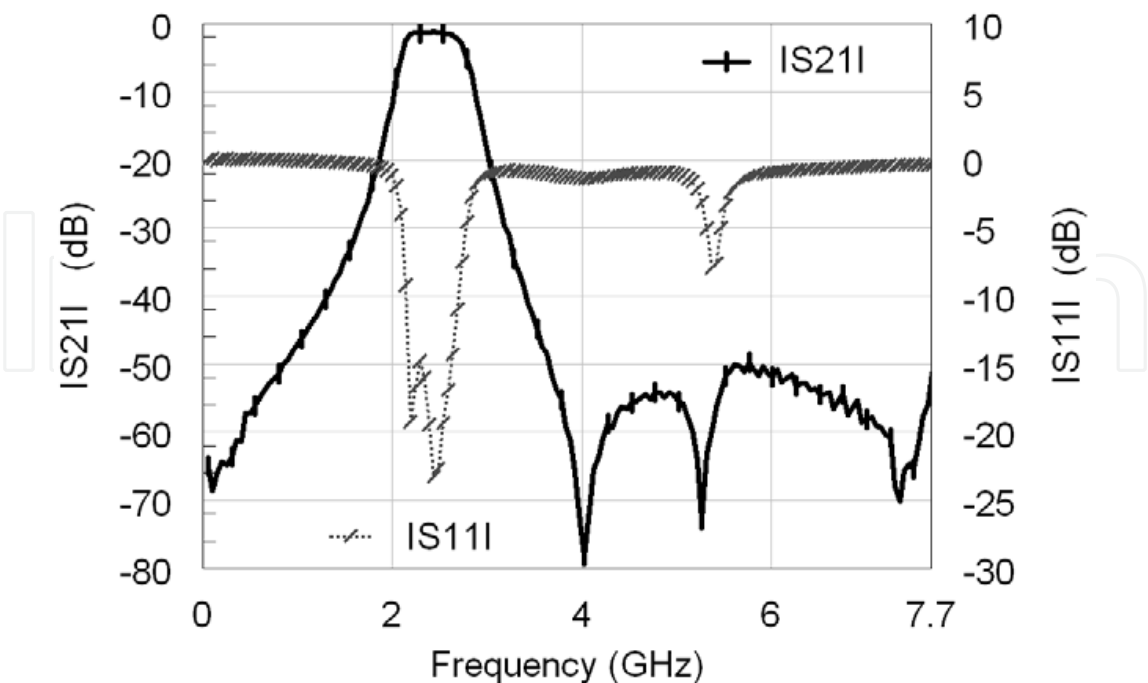


Fig. 16. Measured results of 2.2~2.7GHz low loss WiMAX bandpass filter

b) 3.5GHz WiMAX bandpass filters

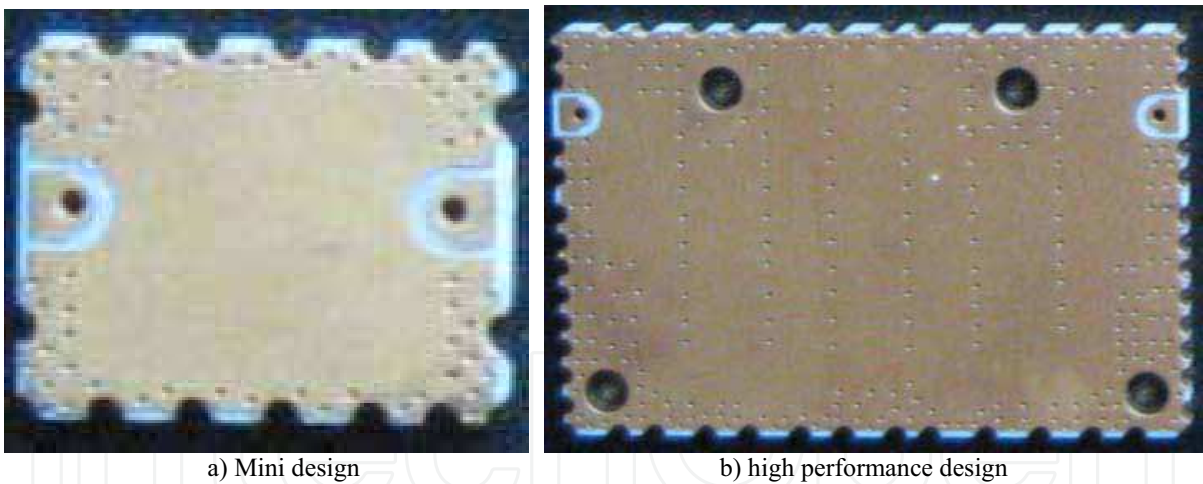


Fig. 17. Photographs of 3.5 GHz WiMAX filter samples

The band pass filter in Figure 17 a) has performances with pass band from 3.3GHz~3.6GHz with minimum insertion loss less than 2dB stop band from 3.7GHz to 7GHz as the measured results shown in Figure 18. The stop band rejection is better than 25dB from 3.7GHz to 7GHz. The band pass filter has much compact size of 11mm X 8.5mm X 1.5 mm³. The other strength for this type filter is surface mounting and self-packaging with low RF radiation.

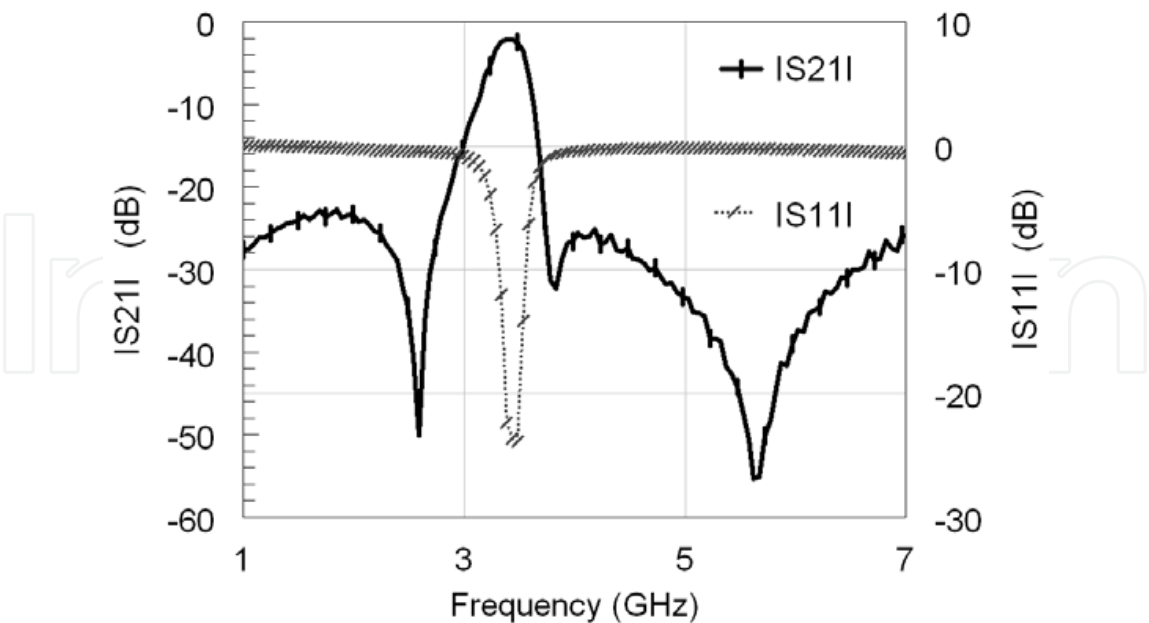


Fig. 18. Measured results of 3.3~3.6GHz mini WiMAX bandpass filter

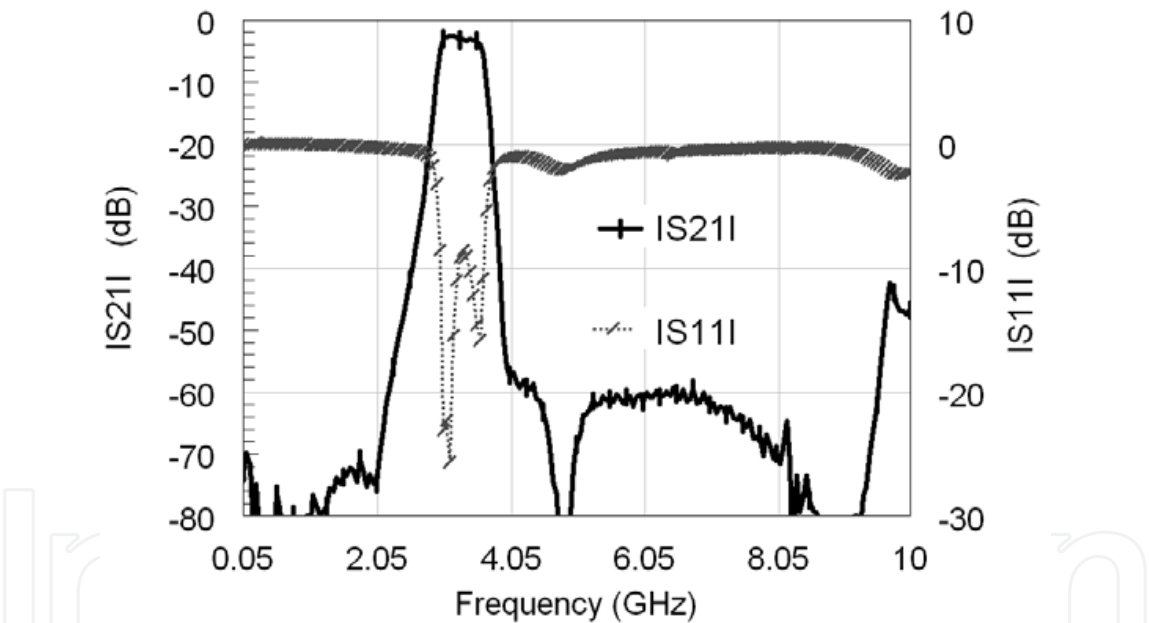


Fig. 19. Measured results of 3.0~3.6GHz high performance WiMax bandpass filter

The band pass filter in Figure 17 b) has performances with pass band from 3.0GHz~3.6GHz with minimum insertion loss of less than 2.5dB and ultra wide stop band from 3.8GHz to 10GHz as shown in Figure 19. The stop band rejection is better than 55dB from 4GHz to 9.5 GHz. The band pass filter has compact size of 25mm X 15mm X 1.5 mm. The other strength is the self-packaging format of surface mounting which is convenient for integration and free of RF leakage.

7. Conclusion

In this Chapter, bandstop filter is investigated based on proposed equivalent circuit model. The 2.4 GHz and 3.5 GHz bandstop filters for WiMAX application are designed and implemented theoretically and experimentally. The important issue of packaging is investigated and an approach to overcome the leakages to improve the performance is adopted. The implemented step impedance resonator section filters with compact size, high stopband rejection, flat group delay and ultra-wide passband bandwidth are used in the new application scenario of WiMAX equipment for nonlinear measurement. It should be addressed that although the filters are designed for WiMAX test equipment, it can also be adopted for other wireless communications with the requirement of rejection in certain range of the frequency 2.3GHz~2.85GHz such as WCS, ISM equipment and MMDS. The recent work on the series of WiMAX bandpass filter developments in 2.4 and 3.5GHz WiMAX bands is also demonstrated for WiMAX applications.

8. Acknowledgment

The authors would like to thank Dr. Dylan Williams for his kind review and constructive advices which make the manuscript more readable. The authors also thank Mr. Yap Kai Meng Leong from ST electronic (Satcom & Sensor) for his help in grammar checking.

9. References

- [1] "IEEE Standard for Local and Metropolitan Area Networks Part 16: Air Interface for Fixed Broadband Wireless Access Systems", *IEEE Std. 802.16-2004*.
- [2] WiMAX Forum. IEEE 802.16a standard and WiMAX igniting broadband wireless access. Whitepaper, May 2004. <http://www.wimaxforum.org>.
- [3] Matthaei G. L., Young L. and Jones E. M. T., *Microwave Filters, Impedance-matching Networks, and Coupling Structures*. Artech House books · Dedham, MA 1964.
- [4] Hong J.-S. and Lancaster M. J., *Microstrip Filters for RF/Microwave Applications*, John Wiley & Sons, Inc. 2001.
- [5] Young L., Matthaei G. L., and Jones E. M. T., "Microwave band-stop filters with narrow stop bands," *IEEE Trans. Microwave Theory Tech.* vol. 12, pp. 416-427, Nov. 1962.
- [6] Schiffman B. M. and Matthaei G. L., "Exact design of band-stop microwave filters," *IEEE Trans. Microwave Theory Tech.* vol. 10, pp. 6-15, Jan. 1964.
- [7] Bell H. C., "L-resonator bandstop filters," *IEEE Trans. Microwave Theory Tech.* vol. 10, pp. 2669-2672, Dec. 1996.
- [8] Qian J.-R. and Zhuang W.-C., "New narrow-band dual-mode bandstop waveguide filters," *IEEE Trans. Microwave Theory Tech.*, vol.31 pp.1045-1050, Dec. 1983.
- [9] Saenz E. M., Subramanyam G., Keuls F. W.V., Chen C., and Miranda F. A., "Fixed-frequency and frequency-agile (Au, HTS) microstrip bandstop filters for L-band applications," *IEEE Trans. Appl. Supercond.*, vol.11 pp.395-398, Mar. 2001.
- [10] Wallage S., Tauritz J. L., Hadley P., Lander L., and Mooij J. E., "High Tc superconducting CPW bandstop filters," *IEEE Microwave and Guided Wave Lett.*, vol. 6 pp.292-294, Aug. 1996.
- [11] Górrur A. and Karpuz C., "Uniplanar compact wideband bandstop filter," *IEEE Microwave and Wireless Components Lett.*, vol. 13, pp. 114-116, Mar. 2003.
- [12] Yang R.-Y., Weng M.-H., Hung C.-Y., Chen H.-J., and Houng M.-P., "Novel compact microstrip interdigital bandstop filters," *IEEE Trans. On Ultrasonics, Ferroelectrics, and Frequency Control.*, vol. 51 pp.1022-1025, Aug. 2004.

- [13] Zhang X. J., Liu A.Q., Karim M. F., Yu A. B. and Shen Z. X., "MEMS-based photonic bandgap (PBG) bandstop filter," *IEEE MTT-S Int. Symp. Dig.*, pp. 1463-1466. 2004.
- [14] Levy R., Snyder R. V. and Shin S., "Bandstop Filters With extended Upper Passbands," *IEEE Trans. Microwave Theory Tech*, vol.54, pp.2503-2515, June, 2006,.
- [15] Ma K., Xiao S.-Q., Chan K.-T., Yeo K. S., Ma J.-G., and Do M. A., "Characterizing and modeling conductor-backed CPW Periodic band stop filter with miniaturized size" *IEEE MTT-S Int. Microwave Symp. Dig.*, pp.983-986, 2007.
- [16] Ma K., Jayasuriya R. M. and Chan K. T., "High Performance Bandstop Filter Design and Investigation Using Physical Model for WiMAX Measurement Equipment," *IEEE MTT-S Int. Microwave Symp. Dig.*, 2008.
- [17] Kim S.-J., Yoon H.-S. and Lee H.-Y., "Suppression of leakage resonance in coplanar MMIC packages using a Si sub-mount layer," *IEEE Trans. Microwave Theory Tech.*, vol. 48, pp. 2664-2669 Dec. 2000.
- [18] Lo Y. T., Tzuang C. C., Peng S. T., Tien C. C., Chang C. C., and Huang J. W., "Resonance phenomena in conductor-backed coplanar waveguides (CBCPW's)," *IEEE Trans. Microwave Theory Tech.*, vol. 41, pp. 2099-2108, DEC. 1993.
- [19] Raskin J.- P., Gauthier G., Katehi, L. P. and Rebeiz G. M., "Mode conversion at GCPW-to-microstrip-line transitions," *IEEE Trans. Microwave Theory Tech.*, vol. 48, pp. 158-161 Jan. 2000.
- [20] Ma K., Ma J.-G., Do M. A., and Yeo K. S., "Experimentally Investigating Slow-Wave Transmission Lines and Filters Based on Conductor-Backed CPW Periodic Cells," *IEEE MTT-S Int. Microwave Symp. Dig.*, pp.1653-1657, 2005.
- [21] Ma K., Yeo K. S., Ma J.-G., and Do M. A., "An Ultra-Compact Planar Band Pass Filter with Open-ground Spirals for Wireless Application" *IEEE Transaction on advanced packaging*, Vol. 31, NO. 2, pp.285-291, May 2008



WIMAX New Developments

Edited by Upena D Dalal and Y P Kosta

ISBN 978-953-7619-53-4

Hard cover, 442 pages

Publisher InTech

Published online 01, December, 2009

Published in print edition December, 2009

WiMAX (Worldwide Interoperability for Microwave Access) is a wireless broadband access network named by industry group called the WiMAX forum formed in June 2001. It is Wireless MAN with IEEE 802.16 family standards. Loosely, WiMAX is a standardized wireless version of Ethernet that enables the last mile, intended primarily as an alternative to wire technologies (such as Cable Modems, DSL and T1/E1 links) to provide broadband access to customer premises. Mission of the WiMAX forum is to promote and certify compatibility and interoperability of broadband wireless products. This book touches most of the above issues in form of 22 individuals' papers containing research work in WiMAX domain in particular. WiMAX has two important standards/usage models: a fixed usage model IEEE 802.16-2004 for Fixed Wireless Broadband Access (FWBA) and a portable usage model IEEE 802.16e-2005, which is mainly concentrated on Mobile Wireless Broadband Access (MWBA). Both are released as standards and amendments are available in form of drafts. Higher data rate transmissions (@ 100 Mbps) are achieved in IEEE 802.16-2004 WiMAX through LOS communications which incorporate a stationary transmitter and receiver but IEEE 802.16e supporting NLOS communication is much complicated and little less bit rate is achieved. 2-11 GHz licensed band is the range of frequencies with TDD and FDD supports. The book will provide a wide horizon to visualize the WiMAX technology and its developments leading towards 4G systems. It will provide a good platform to the researchers with clues to the innovative ideas in WiMAX domain. I wish all the best to the authors and readers of this book in their successful research of WiMAX technology.

How to reference

In order to correctly reference this scholarly work, feel free to copy and paste the following:

Kaixue Ma, Leyu Zhang and Kiat Seng Yeo (2009). Advanced Filter Development for WiMAX Applications, WIMAX New Developments, Upena D Dalal and Y P Kosta (Ed.), ISBN: 978-953-7619-53-4, InTech, Available from: <http://www.intechopen.com/books/wimax-new-developments/advanced-filter-development-for-wimax-applications>

INTECH
open science | open minds

InTech Europe

University Campus STeP Ri
Slavka Krautzeka 83/A
51000 Rijeka, Croatia
Phone: +385 (51) 770 447

InTech China

Unit 405, Office Block, Hotel Equatorial Shanghai
No.65, Yan An Road (West), Shanghai, 200040, China
中国上海市延安西路65号上海国际贵都大饭店办公楼405单元
Phone: +86-21-62489820

www.intechopen.com

Fax: +385 (51) 686 166
www.intechopen.com

Fax: +86-21-62489821

IntechOpen

IntechOpen

© 2009 The Author(s). Licensee IntechOpen. This chapter is distributed under the terms of the [Creative Commons Attribution-NonCommercial-ShareAlike-3.0 License](https://creativecommons.org/licenses/by-nc-sa/3.0/), which permits use, distribution and reproduction for non-commercial purposes, provided the original is properly cited and derivative works building on this content are distributed under the same license.

IntechOpen

IntechOpen